

This is the accepted manuscript made available via CHORUS. The article has been published as:

## Particle decay of proton-unbound levels in $^{12}\text{N}$

K. A. Chipps, S. D. Pain, U. Greife, R. L. Kozub, C. D. Nesaraja, M. S. Smith, D. W. Bardayan, A. Kontos, L. E. Linhardt, M. Matos, S. T. Pittman, and P. Thompson (JENSA Collaboration)

Phys. Rev. C **95**, 044319 — Published 24 April 2017

DOI: [10.1103/PhysRevC.95.044319](https://doi.org/10.1103/PhysRevC.95.044319)

# Particle Decay of Proton-Unbound Levels in $^{12}\text{N}$

K.A. Chipps,<sup>1</sup> S.D. Pain,<sup>1</sup> U. Greife,<sup>2</sup> R.L. Kozub,<sup>3</sup> C.D. Nesaraja,<sup>1</sup> M.S. Smith,<sup>1</sup> D.W. Bardayan,<sup>4</sup> A. Kontos,<sup>5,6</sup> L.E. Linhardt,<sup>7</sup> M. Matos,<sup>1</sup> S.T. Pittman,<sup>8</sup> and P. Thompson<sup>8</sup>

(The JENSA Collaboration)

<sup>1</sup>*Oak Ridge National Laboratory, Oak Ridge, TN 37831*

<sup>2</sup>*Colorado School of Mines, Golden, CO 80401*

<sup>3</sup>*Tennessee Technological University, Cookeville, TN 38505*

<sup>4</sup>*University of Notre Dame, Notre Dame, IN 46556*

<sup>5</sup>*National Superconducting Cyclotron Laboratory and  
Michigan State University, East Lansing, MI 48824*

<sup>6</sup>*Joint Institute for Nuclear Astrophysics (JINA),  
University of Notre Dame, Notre Dame, IN 46556*

<sup>7</sup>*Louisiana State University, Baton Rouge, LA 70803*

<sup>8</sup>*University of Tennessee, Knoxville, TN 37996*

# Abstract

**Background** Transfer reactions are a useful tool for studying nuclear structure, particularly in the regime of low level densities and strong single-particle strengths. In addition, transfer reactions can populate levels above particle decay thresholds, allowing for the possibility of studying the subsequent decays and furthering our understanding of the nuclei being probed. In particular, the decay of loosely bound nuclei such as  $^{12}\text{N}$  can help inform and improve structure models.

**Purpose** To learn about the decay of excited states in  $^{12}\text{N}$ , to more generally inform nuclear structure models, particularly in the case of particle-unbound levels in low-mass systems which are within the reach of state-of-the-art ab initio calculations.

**Method** In this follow-up analysis of previously published data [1], decay particles from excited states populated in  $^{12}\text{N}$  have been detected in coincidence with tritons from the  $^{14}\text{N}(\text{p},\text{t})^{12}\text{N}$  transfer reaction. Specifically, decay protons from proton-unbound levels above  $\sim 2$  MeV excitation energy were observed by utilizing the Jet Experiments in Nuclear Structure and Astrophysics (JENSA) gas jet target.

**Results** Isotropic proton branching ratios for the p0 and p1 decay channels are calculated and decay particle spectra for the populated levels from p0, p1, and p2 decay are given.

**Conclusions** The current data from  $^{14}\text{N}(\text{p},\text{t})^{12}\text{N}$  will help provide nuclear structure and decay information input to models in this mass region.

PACS numbers:

## I. INTRODUCTION

Transfer reactions have long been used to populate levels above the particle decay thresholds in nuclei of interest, both in normal and inverse kinematics. In some circumstances, it is desirable to measure not only the energy, spin-parity, or spectroscopic information of these levels, but the properties of their decay (see, for example, Refs. [2–8], for a range of such studies). In inverse kinematics, the decay particles are given the additional momentum kick from the beam, minimizing the energy differences between reaction products and decay particles. In the case of particle decay from normal kinematics reactions, however, a technical problem arises: how to simultaneously measure the relatively high energies of reaction products and the very low energies of coincident decay particles. In previous measurements, this issue has been addressed by measuring reaction and decay products in separate arrays or arrangements of charged-particle detectors (see, for example, references [5, 9–11]).

In addition to the difficulty in detecting a wide dynamic range, the targets themselves can prevent reaction-decay coincidence measurements. If a target is thick, particularly due to gas cell windows or backing foils, decay particles may not have sufficient energy to escape, and those that do suffer from considerable worsening in resolution due to straggling. Targets which contain chemical mixtures, such as plastic foils (for example,  $\text{CH}_2$ ), may also hinder coincidence measurements if the unwanted component creates too much beam-induced background (for example, if elastic scattering of carbon in  $\text{CH}_2$  swamps the detection of low-energy decay products from the compound nucleus near  $90^\circ$ ).

The main goal of this experiment had been the search for excited states in  $^{12}\text{N}$  and was published as Ref. [1]. In the current work, reaction products and decays from excited, particle-unbound levels populated in  $^{14}\text{N}(\text{p},\text{t})^{12}\text{N}^* \rightarrow \text{p} + ^{11}\text{C}$  are serendipitously detected in the same detectors, with improved resolution due to improved target purity. Because this analysis was a byproduct measurement there is room for improvement in the technique. It is here presented as an example of the potential for this kind of study, particularly with pure and localized gas targets.

Excited levels in  $^{12}\text{N}$  have been the focus of many studies over the years [1, 3, 12–25], but without much (if any) focus on the decay of those levels. The breakup of excited states in  $^{12}\text{N}$  has been examined previously [25], as has the reverse reaction ( $^{11}\text{C} + \text{p}$  resonant scattering [21]), but with the explicit goal of informing the astrophysical  $^{11}\text{C}(\text{p},\gamma)^{12}\text{N}$  reaction rate

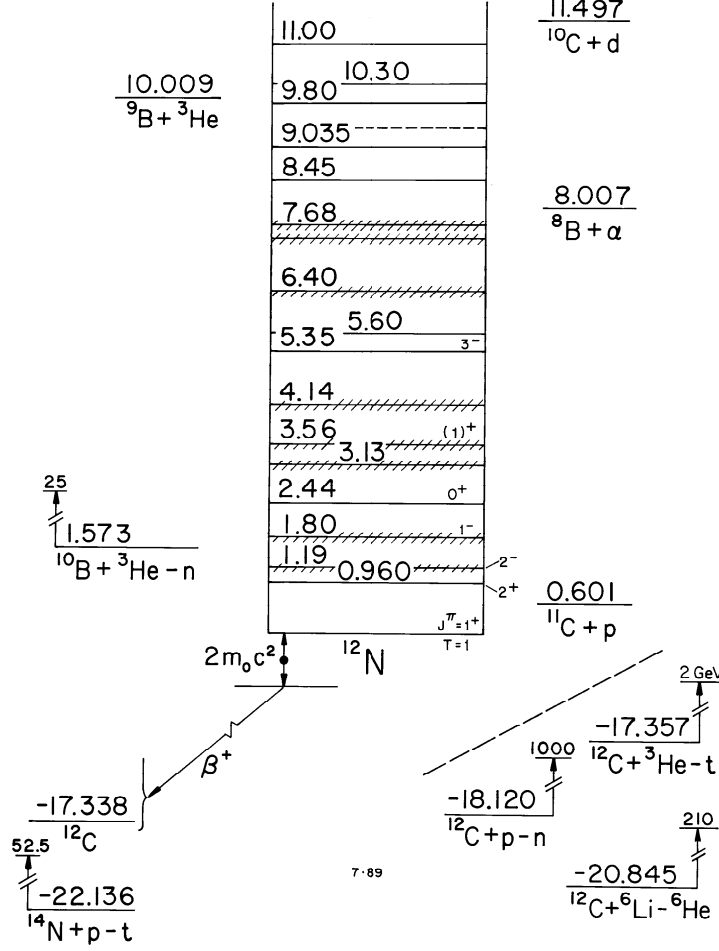


FIG. 1: Energy level diagram for  $^{12}\text{N}$ , from the 1990 evaluation by F. Ajzenberg-Selove [26]. The particle decay thresholds for  $^{11}\text{C} + \text{p}$  and  $^8\text{B} + \alpha$  are shown on the right.

relevant for potential  $3\alpha$  reaction bypass paths and hence focusing on the first two excited states in  $^{12}\text{N}$ . The current study extends to higher excitation energies (a level diagram for  $^{12}\text{N}$  is shown in Figure 1). Two previous measurements [3, 17] of the  $^{12}\text{C}(^3\text{He}, \text{t})^{12}\text{N}$  reaction observed coincident proton decays from excited levels in  $^{12}\text{N}$ ; comparisons with the current work are discussed below.

## II. EXPERIMENT

The setup used for the current measurement is identical to that described in Ref. [1]. In brief, a jet of 300 psig ( $\sim 5 \times 10^{18}$  atoms/cm $^2$ )  $^{nat}\text{N}$  was produced with the Jet Experiments in Nuclear Structure and Astrophysics (JENSA) gas jet target system [27] and bombarded by

a 38 MeV proton beam of  $\sim 1\text{-}4$  enA from the Holifield Radioactive Ion Beam (HRIBF) 25 MV tandem accelerator. Around the target were three  $\Delta E$ -E telescopes of SIDAR (Micron YY1) annular strip detectors in “lampshade” mode [28] covering laboratory angles of  $\sim 19\text{-}54^\circ$  degrees. The detectors were calibrated with an alpha source of known activity.

Using the initial  $\Delta E$ -E particle ID method to identify tritons originating from the  $^{14}\text{N}(p,t)^{12}\text{N}$  reaction as described in Ref. [1], particles which fell within a timing gate of roughly  $6\text{ }\mu\text{s}$  from the initial triton hit, but not in the same detector as the triton hit, were considered to be coincident<sup>1</sup>. The sum ( $\Delta E + E$ ) energy of the coincident particles was plotted against triton energy to search for decay particles from the residual nucleus created by the (p,t) reaction. This technique is demonstrated in Figure 2. Several diagonal bands of true coincident particles can be seen, tending toward the proton threshold in  $^{12}\text{N}$  along lines of constant  $E_x + E_r$ . Because no other particle thresholds exist between  $S_p$  (0.601 MeV) and  $S_\alpha$  (8.008 MeV) in  $^{12}\text{N}$  [26], the coincident particles seen in the bands in Fig. 2 must be protons<sup>2</sup>.

Due to the thresholds set in the data acquisition hardware and firmware for the original measurement, coincidences were only detectable down to a decay proton energy of about 750 keV, or above the second excited state in  $^{12}\text{N}$  if the p0 decay channel (to the  $^{11}\text{C}$  ground state) is considered<sup>3</sup>. This also means that the “turn on” energy for each decay channel as detected is a convolution of both the particle decay threshold and the experimental threshold, though the experimental threshold is roughly constant, and the level spacing of the first three states in  $^{11}\text{C}$  is also reasonably constant ( $\sim 2$  MeV). The experimental threshold also includes a cutoff to account for a large number of random coincidences near the strongly-populated ground state, which is due to the wide timing gate in conjunction with a high beam intensity (up to 4 nA); in future measurements, a tighter timing requirement would greatly reduce this background. As is evident from Fig. 2, multiple decay channels are present, namely, the p0, p1, and p2 channels to the ground, first, and second excited states in  $^{11}\text{C}$ , respectively. The ground state of  $^{11}\text{C}$  is  $\frac{3}{2}^-$ .

---

<sup>1</sup> The requirement that the coincidence be in a different detector telescope, while hurting the coincidence efficiency, removed any background from self-counting and/or crosstalk.

<sup>2</sup> The total thickness of silicon detector in this case is around 1.1mm, so we are not sensitive to betas above about half an MeV.

<sup>3</sup> The thresholds of the gates seen in Fig. 2 are  $\sim 750$  keV for p0,  $\sim 1.5$  MeV for p1, and  $\sim 2.5$  MeV for p2.

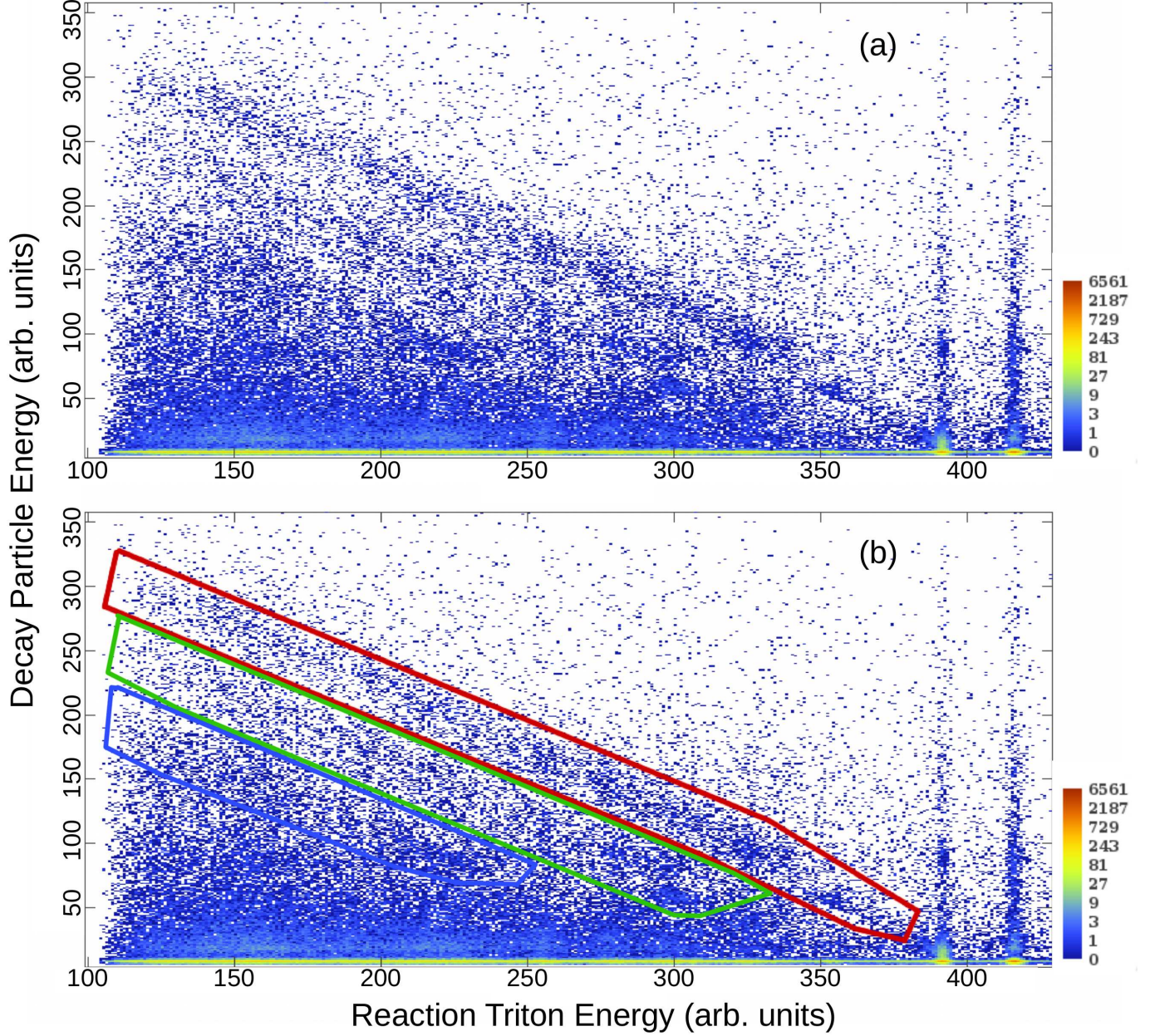


FIG. 2: (Color online) 2D spectrum of triton energy (abscissa, arb. units) versus the energy of any particle detected in coincidence in any other detector telescope (ordinate, arb. units). Both axes are approximately 30 keV per channel. In panel (a), several lines of coincidences due to particle decay can be clearly seen, trending toward the proton threshold around channel 380. Due to the high rate of random coincidences near the ground and first excited states (to the right of the figure), the coincidence gate could not be reliably extended into this region (see text). Panel (b) shows the same spectrum with the coincidence gates corresponding to p0 (red, upper), p1 (green, middle), and p2 (blue, lower) overlaid.

### III. ANALYSIS

#### A. Proton-gated triton spectra

Projecting the gates in Figure 2 onto the triton energy axis, summing over all angles<sup>4</sup>, and correcting for geometric detection efficiency resulted in the decay-gated triton spectra shown in the top panel of Fig. 3. The triton singles spectrum is shown in black, and tritons gated on coincident decays are shown in red (p0), green (p1), and blue (p2), the colors corresponding to the gates in the triton energy vs decay energy plot (bottom panel of Fig. 2). These decay-gated triton spectra are corrected only for geometric efficiency; a discussion of anisotropy appears in Section III C. Again, the energy at which each proton decay channel begins is due to both the actual decay energy threshold and the hardware/firmware thresholds. The results from a gate of the same size but offset from any of the correlated triton-decay energy bands is shown as a background estimate in brown. The isotropic branching ratio “strength function” in the bottom three panels of Fig. 3 were calculated from the bin-by-bin ratio of the decay-gated to ungated (singles) spectra after background subtraction.

For the p0 and p1 channels, some structure is apparent, so individual peaks can be fitted for a more accurate proton branching ratio. Table I and Figure 4 show the efficiency-corrected, isotropic branching ratios from the different levels populated in  $^{12}\text{N}$ . The adopted uncertainties include both a statistical component and an estimated systematic uncertainty arising from variations in detector position (and hence efficiency), target thickness, goodness of the (Gaussian) fit, and the assumption of isotropy. The p2 channel, as it did not display any obvious structure in the decay-gated triton spectra, was not considered.

#### B. Decay proton spectra

Though the statistics were limited, spectra of the decay protons themselves could be produced by projecting the gates in Figure 2 onto the decay energy axis (summed over all angles), as is shown in Fig. 5. It is apparent that the resolution of the decay particle spectra is somewhat worse than the triton singles spectra, as is expected due to greater energy straggling in the target,  $\Delta E$  detector, and detector dead layers of the lower energy particles.

---

<sup>4</sup> The spectra were all adjusted in energy to match a single angle for summing purposes.



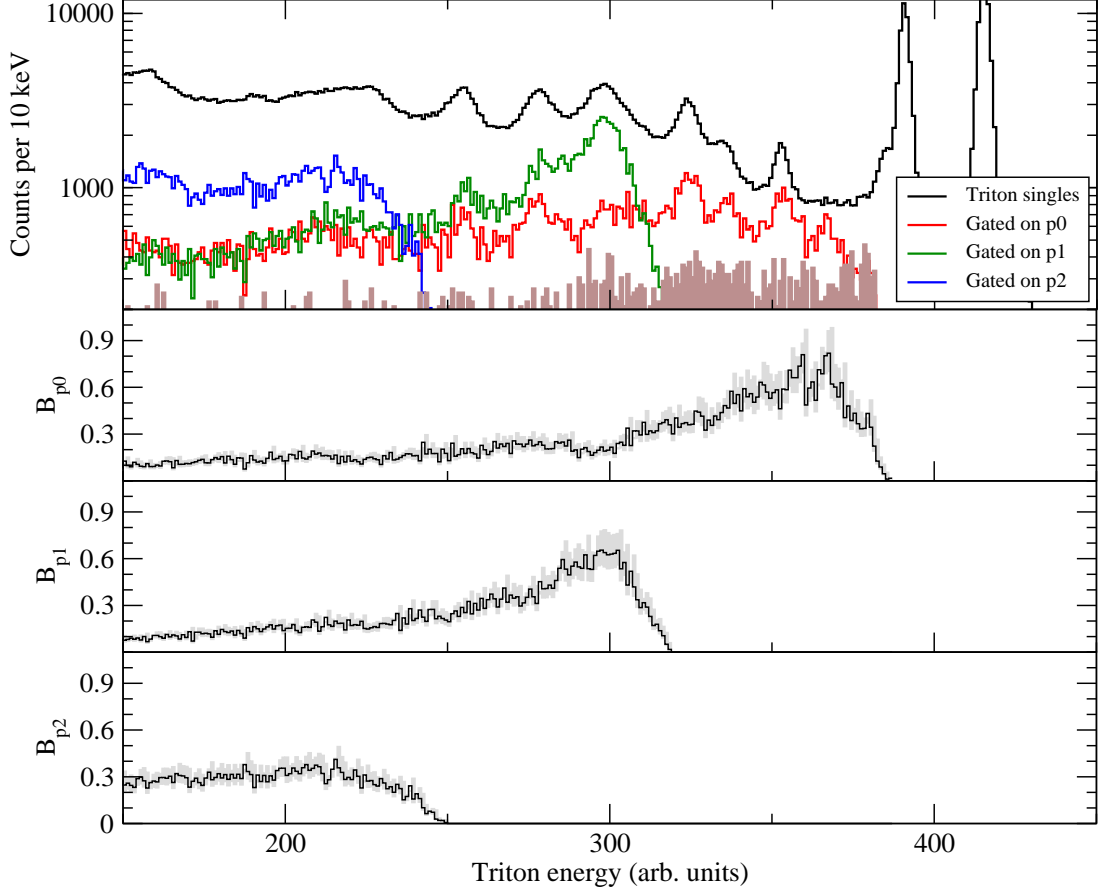


FIG. 3: (Color online) Top panel: triton singles energy spectrum summed over all angles (black; compare with Fig. 2 of Ref. [1]) overlaid with the summed triton spectrum gated on decay particle coincidences (red for p0, farthest right greyscale curve; green for p1, middle greyscale curve; and blue for p2, farthest left greyscale curve; as in Fig. 2), corrected only for detection efficiency. The result of a similarly-sized gate off the coincident particle bands is shown in solid brown. Bottom three panels: the isotropic proton branching ratio strength function (black) derived from the ratio of the gated and ungated spectra shown above for each of the decay branches (p0, p1, p2), as indicated by the axis labels. The grey band indicates the combined uncertainty due to statistics and the efficiency calibration.

Using the external (alpha source) and internal (known  $^{12}\text{N}$  levels) calibrations [1] for each detector gives the approximate energies of the observed decay-proton peaks<sup>5</sup>, listed in Table

<sup>5</sup> Possible nonlinearities in the calibration at very low energies, as well as differences in energy loss and ballistic deficit between different particle types, are not accounted for here.

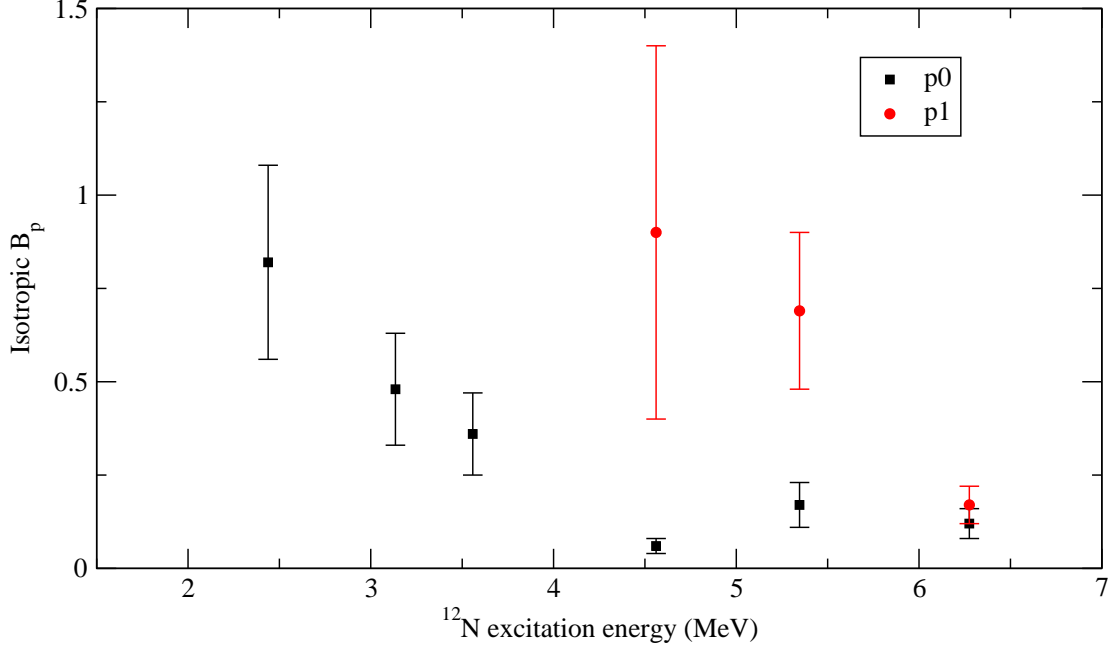


FIG. 4: (Color online) Branching ratios extracted for the different  $^{12}\text{N}$  levels populated in the current work, assuming isotropic proton decay. Some allowed decays are not observed due to detector thresholds and low statistics. Observation of p2 decay to any discrete levels could not be confirmed, and hence is not included. Uncertainties include statistics and a 30% systematic uncertainty to account for the possible anisotropy (see text).

II. Not all allowed decays are discernible in the spectra due to the high thresholds, low statistics, and worsened energy resolution. As before, the p2 channel is ignored due to the lack of information, though it is worth noting that the decay proton from a broad state at  $\sim 7.4$  MeV to the second excited state in  $^{11}\text{C}$  ( $E_p \simeq 2.48$  MeV) would fall near the detection threshold for this channel ( $\sim 2.56$  MeV), so this may be the structure seen at the far left of the p2 spectrum in the bottom panel of Fig. 5. The decay proton peaks line up reasonably well with known transitions, providing additional weight to the assignment of these proton decays, and in particular bolstering the assignment of the previously unobserved level at 4.561 MeV excitation energy to  $^{12}\text{N}$  [1].

TABLE I: Proton decay from  $^{12}\text{N}$  levels populated by  $^{14}\text{N}(\text{p,t})$ . Isotropic decay is assumed in the calculation of branching ratios, but the uncertainties include a systematic component of 30% to account for discrepancy from anisotropy; see text. The p2 channel is not included, as it did not display any reliable structure for fitting of individual levels.

$E_x^a$ (MeV)	$J^\pi$	Isotropic $B_{p0}$	Isotropic $B_{p1}$
$2.438 \pm 0.016$	$0^+$	$0.82 \pm 0.26$	
$3.135 \pm 0.019$	$2^+$	$0.48 \pm 0.15$	
$3.558 \pm 0.007$	$1^+$	$0.36 \pm 0.11$	
$4.561 \pm 0.024$	$(1,2)^+$	$0.06 \pm 0.02$	$0.90 \pm 0.50^b$
$5.346 \pm 0.009$	$(1,2,3)^+$	$0.17 \pm 0.06$	$0.69 \pm 0.21$
$6.275 \pm 0.021$	$(1^-3^+)$ ,	$0.12 \pm 0.04$	$0.17 \pm 0.05$

<sup>a</sup> Excitation energies and spin/parity assignments from Ref. [1].

<sup>b</sup> This branching ratio includes an additional 46% systematic uncertainty due to potential pileup in the lowest energy portion of the p1 gate.

TABLE II: Measured decay proton energies for p0 and p1 from the decay proton spectra, compared with expectation, adopting the  $^{11}\text{C}+\text{p}$  threshold of 0.601 MeV [26] and level energies from Ref. [1]. Uncertainties include the experimental resolution for detection of decay protons, and goodness of fit; uncertainties on the expected transitions are on the order of ten keV. The p2 channel is not included. Because of statistics and worsened energy resolution, not all transitions are observed in the decay proton spectra which can be observed in the proton-gated triton spectra (see text).

Channel	Transition	$E_p$ (MeV), expected	$E_p$ (MeV), measured
p0	$2.438 \rightarrow 0.00$	1.837	$1.97 \pm 0.53$
p0	$3.558 \rightarrow 0.00$	2.957	$3.36 \pm 0.75$
p1	$4.561 \rightarrow 2.00$	1.960	$2.11 \pm 0.67$
p1	$5.346 \rightarrow 2.00$	2.745	$3.35 \pm 2.09$

### C. Angular correlations and anisotropy

While it is, to first order, expected that the decays from unbound levels in  $^{12}\text{N}$  will be anisotropic, the current measurement, due to limited statistics, did not have sufficient sensi-

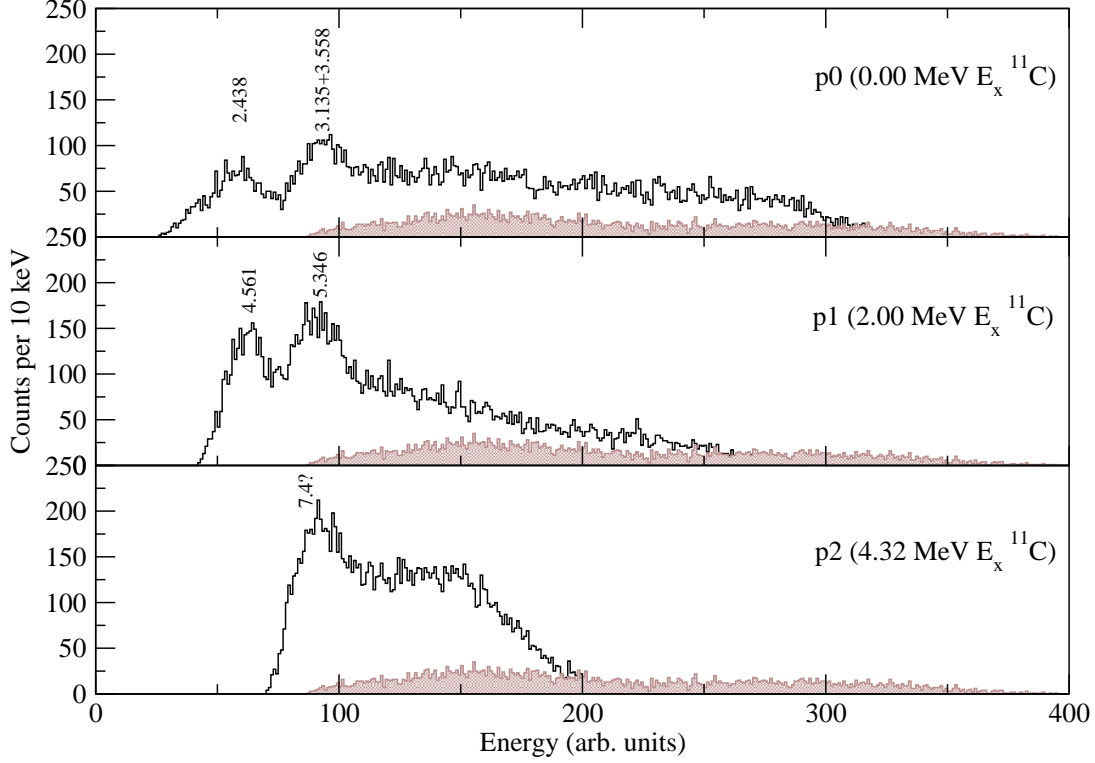


FIG. 5: (Color online) The (p,t)-coincident p0 (top panel), p1 (middle panel), and p2 (bottom panel) decay spectra (summed over all angles). The brown shaded area in each panel corresponds to the background as determined by a gate outside the area of reaction-decay coincidences (cf. Fig. 2). Prominent peaks are labeled with the excitation energy of the  $^{12}\text{N}$  level from which they originated; see also Table II.

tivity to derive angular correlations between the reaction triton and decay proton. Therefore, all of the branching ratios tabulated above are derived based on an assumption of isotropy, with a conservative 30% systematic uncertainty included to account for discrepancies between isotropic and anisotropic decay over the angular range covered, based on previous measurements [9, 10].

In order to observe whether there was any anisotropy in the data without relying on spin assignments or angular correlations, a simple test was implemented. Because the center of mass and laboratory frames in the case of normal kinematics differ little, isotropic decay in the center of mass can be modeled as essentially isotropic decay in the laboratory frame. By (geometrically) considering all possible combinations of detector strip hits - for example, a triton from the (p,t) reaction might hit strip 1 while the correlated decay proton hit strip

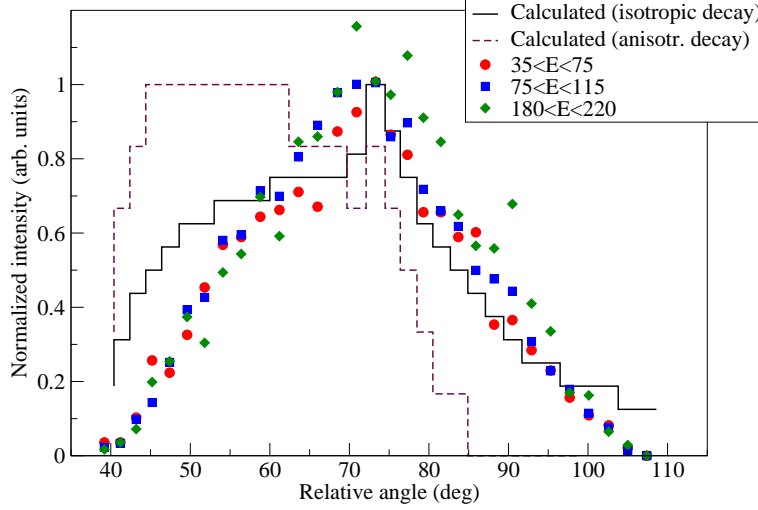


FIG. 6: (Color online) The intensity of p0 decay protons falling within three energy ranges (cf. Fig. 5, corresponding to the first and second spectrum peaks and an area without obvious structure; arbitrary units) is plotted against calculated intensity curves for isotropic (black solid) and an example anisotropic (maroon dashed) decay, as a function of the relative laboratory angle between the decay proton and reaction triton.

2 of the opposite detector in the array - a histogram of relative angle for isotropic decay can be generated, as in Figure 6. An example of anisotropic decay in the laboratory frame, as there are many different possible variations, is a cosine variation in the relative angle; this is also plotted in Fig. 6 for comparison. Three energy ranges of the p0 decay proton were considered for demonstration purposes, making cuts on the channel number shown in the top panel of Fig. 5, and the relative angles calculated on an event-by-event basis. It is apparent from comparison with the theoretical curves in Fig. 6 that the p0 proton decay is largely isotropic. This reasonably justifies the assumption of isotropy when extracting the branching ratios, as any adjustment to account for anisotropy must be small.

Applying this technique in the future, providing a larger angular coverage of detectors will help in “washing out” the differences between isotropic and anisotropic decays, as a larger percentage of  $4\pi$  would be included. Additional statistics would allow for angular correlation measurements to be made.

## IV. DISCUSSION

Nuclear structure considerations indicate that the unbound levels of  $^{12}\text{N}$  (everything above the ground state) should have large proton decay branching ratios, and overall this is what is observed in the current measurement. This is consistent with the proton decay seen in the  $^{12}\text{C}(^3\text{He},t)^{12}\text{N}$  charge exchange reaction study. Branching ratios consistent with unity about an MeV above the threshold slowly decrease in value until the next proton decay channel opens, and the process repeats itself. The p2 channel is also expected to display this behavior, until the  $\alpha$  decay channel becomes energetically favorable; unfortunately the current measurement was not sensitive to these channels. Proton decays to the third excited state in  $^{11}\text{C}$  (around 4.8 MeV [26]) were not observed. Thanks in part to the large angular coverage of the SIDAR detectors placed close to the JENSA gas jet target, the correction for anisotropic decay appears to be small, and likely does not affect the general trends in the measured branching ratios. The relatively flat angular correlation measurements of Ref. [3] appear to support this conclusion.

The charge exchange reaction studies of Sterrenburg *et al.* [17] of Inomata *et al.* [3] also observed the p0, p1, and (p2+p3) channels (Ref. [3] did not claim sufficient resolution to separate decays to the 4.319 and 4.804 MeV levels in  $^{11}\text{C}$ ), and in the case of Ref. [3] to higher  $^{12}\text{N}$  excitation energies than the current work due to the high bombarding energies and thick charged particle detectors used. The decay-proton-coincident spectra from those works (cf. Figure 14 of Ref. [3] or Figure 5 of Ref. [17]) display the same behavior as in the current work: peak structure at lower decay energies, followed by a continuum of decreasing strength. Both of the previous works assessed the angular correlations of the decay protons and reaction tritons on a region-by-region (gating bins) basis, instead of fitting individual peak structures. The experimental resolution (350 - 450 keV [3]) prevents an accurate comparison between the broad ( $\sim 1.4$  MeV wide) structure seen between 4 and 5 MeV in the previous measurements [3, 17] and the previously unreported level at 4.561 MeV in the current work. However, in both cases, the authors note that the behavior of a half-width bin on one side or the other of that broad peak do not display the same shape, indicating that the structure contains multiple spin/parity contributions. In addition, the decay-proton-gated triton spectra of Inomata *et al.* [3] seem to indicate the broad structure at  $\sim 4$  MeV decaying via two separate modes (p0 and p1) from two separate parent levels;

in the current work, no such split is observed for the 4.561 MeV level, indicating that the (p,t) reaction populates a different subset of the levels inside that broad 4-5 MeV excitation energy structure than the ( $^3\text{He}$ ,t) charge exchange reaction does.

Spectra of the decay protons from the current work, while statistics limited, displayed several clear peaks corresponding to known decays. In particular, several strong decay channels from the 2.438 and 3.558 MeV states in  $^{12}\text{N}$  to the ground state of  $^{11}\text{C}$  and the 4.561 and 5.346 MeV levels in  $^{12}\text{N}$  to the first excited state of  $^{11}\text{C}$  were observed. These decays lend additional weight to the assignment of the 4.561 MeV level as a previously unobserved state in  $^{12}\text{N}$  [1]. It is possible that the structure seen in the p2 decay proton spectrum is due to decays from a broad level around 7.4 MeV excitation energy in  $^{12}\text{N}$  to the second excited state in  $^{11}\text{C}$ , but this assignment is only tentative due in large part to the lack of information on the parent  $^{12}\text{N}$  level. The previous decay measurements [3, 17] did not calculate purely experimental branching ratios for the observed proton decays, as their goal was to inform the nature of the Giant Dipole and Spin Dipole resonances.

Future measurements of this type would benefit greatly from several improvements over the current setup. First, hardware, firmware, and software thresholds should be set much lower, to account for the small signals originating from low energy decay products; the use of digital electronics to separate large-signal reaction products from small-signal decay particles prior to waveform filtering could prove helpful in this regard as well. Second, steps should be taken to reduce the background due to accidental coincidences within the timing window, such as a TAC gate or time-stamping. Third, increased geometric efficiency through the use of large arrays of charge particle detectors will improve statistics and allow for angular correlations between reaction product and decay particle to be measured. Some development along these lines is ongoing (see, for example, Ref. [29]). However, despite the current measurement being originally designed and instrumented for a different purpose, due to the intense proton beam and pure, localized  $^{14}\text{N}$  gas jet target from JENSA, decay particles corresponding to several excited levels in  $^{12}\text{N}$  were observed.

## V. CONCLUSION

The technique of detecting low-energy decay particles from unbound levels in coincidence with the higher-energy reaction products originating from the reaction that populated those

levels is useful for studying the properties of nuclear levels and the properties of their decay. The technique could potentially be used to study particle unbound levels across the nuclear chart, though such measurements require careful setup. Detection of decay particles and reaction products together may also benefit from combined detector technologies, such as a gas-filled detector backed by a silicon detector, to account for the wide dynamic range and help push detection thresholds even lower. Improvements in targetry, such as the use of a thin and localized gas jet, also provide unique gains for the application of this technique. The current work, while not optimized for such a study, demonstrates the feasibility of the method by extracting information on the proton decays from excited, unbound levels in  $^{12}\text{N}$ . In the current work, branching ratios were measured and new structure information on  $^{12}\text{N}$  was acquired.

## Acknowledgments

The authors wish to thank the dedicated staff of the Holifield Radioactive Ion Beam Facility (HRIBF). Author KAC wishes to thank M. Bertolli for assistance in preparing print-ready 2D histograms and W.A. Peters for a careful reading of this manuscript. Research sponsored by the Laboratory Directed Research and Development Program of Oak Ridge National Laboratory, managed by UT-Battelle, LLC, for the U.S. Department of Energy. This work was supported by U.S. Department of Energy, NNSA, and National Science Foundation.

- 
- [1] K. A. Chipps, S. D. Pain, U. Greife, R. L. Kozub, D. W. Bardayan, J. C. Blackmon, A. Kontos, L. E. Linhardt, M. Matos, S. T. Pittman, et al. (JENSA Collaboration), *Phys. Rev. C* **92**, 034325 (2015).
  - [2] W. Catford, E. Garman, and L. Fifield, *Nuclear Physics A* **417**, 77 (1984).
  - [3] T. Inomata, H. Akimune, I. Daito, H. Ejiri, H. Fujimura, Y. Fujita, M. Fujiwara, M. N. Harakeh, K. Ishibashi, H. Kohri, et al., *Phys. Rev. C* **57**, 3153 (1998), URL <http://link.aps.org/doi/10.1103/PhysRevC.57.3153>.
  - [4] J. C. Chow, J. D. King, N. P. T. Bateman, R. N. Boyd, L. Buchmann, J. M. D'Auria, T. Davinson, M. Dombsky, E. Gete, U. Giesen, et al., *Phys. Rev. C* **66**, 064316 (2002).



- [5] C. M. Deibel, J. A. Clark, R. Lewis, A. Parikh, P. D. Parker, and C. Wrede, *Phys. Rev. C* **80**, 035806 (2009).
- [6] A. Raduta, B. Borderie, E. Geraci, N. L. Neindre, P. Napolitani, M. Rivet, R. Alba, F. Amorini, G. Cardella, M. Chatterjee, et al., *Physics Letters B* **705**, 65 (2011).
- [7] R. J. Charity, J. M. Elson, J. Manfredi, R. Shane, L. G. Sobotka, B. A. Brown, Z. Chajecki, D. Coupland, H. Iwasaki, M. Kilburn, et al., *Phys. Rev. C* **84**, 014320 (2011).
- [8] J. Li, Y. L. Ye, Z. H. Li, C. J. Lin, Q. T. Li, Y. C. Ge, J. L. Lou, Z. Y. Tian, W. Jiang, Z. H. Yang, et al., *Phys. Rev. C* **95**, 021303 (2017).
- [9] K. A. Chipps, D. W. Bardayan, K. Y. Chae, J. A. Cizewski, R. L. Kozub, J. F. Liang, C. Matei, B. H. Moazen, C. D. Nesaraja, P. D. O'Malley, et al., *Phys. Rev. C* **82**, 045803 (2010).
- [10] K. A. Chipps, D. W. Bardayan, K. Y. Chae, J. A. Cizewski, R. L. Kozub, C. Matei, B. H. Moazen, C. D. Nesaraja, P. D. O'Malley, S. D. Pain, et al., *Phys. Rev. C* **86**, 014329 (2012).
- [11] C.M. Deibel, Ph.D. thesis, Yale University (2008).
- [12] K.Sugimoto, K.Nakai, K.Matuda, T.Minamisono, *J. Phys. Soc. Japan* **25**, 1258 (1968).
- [13] G. C. Ball and J. Cerny, *Phys. Rev.* **177**, 1466 (1969), URL <http://link.aps.org/doi/10.1103/PhysRev.177.1466>.
- [14] H. Fuchs, K. Grabisch, D. Hilscher, U. Jahnke, H. Kluge, T. Masterson, and H. Morgenstern, *Nuclear Physics A* **234**, 61 (1974), ISSN 0375-9474, URL <http://www.sciencedirect.com/science/article/pii/0375947474903790>.
- [15] C. F. Maguire, D. L. Hendrie, D. K. Scott, J. Mahoney, and F. Ajzenberg-Selove, *Phys. Rev. C* **13**, 933 (1976), URL <http://link.aps.org/doi/10.1103/PhysRevC.13.933>.
- [16] D. E. Alburger and A. M. Nathan, *Phys. Rev. C* **17**, 280 (1978), URL <http://link.aps.org/doi/10.1103/PhysRevC.17.280>.
- [17] W. Sterrenburg, M. Harakeh, S. V. D. Werf, and A. V. D. Woude, *Nuclear Physics A* **405**, 109 (1983), ISSN 0375-9474, URL <http://www.sciencedirect.com/science/article/pii/0375947483903263>.
- [18] M. Harakeh, H. Akimune, I. Daito, Y. Fujita, M. Fujiwara, M. Greenfield, T. Inomata, J. Jnecke, K. Katori, S. Nakayama, et al., *Nuclear Physics A* **577**, 57 (1994), ISSN 0375-9474, proceeding of the International Symposium on Spin-Isospin Responses and Weak Processes in Hadrons and Nuclei, URL <http://www.sciencedirect.com/science/article/pii/0375947494908346>.

- [19] B.D. Anderson *et al.*, Phys. Rev. C **54**, 237 (1996).
- [20] T. Teranishi, S. Kubono, S. Shimoura, M. Notani, Y. Yanagisawa, S. Michimasa, K. Ue, H. Iwasaki, M. Kurokawa, Y. Satou, et al., Physics Letters B **556**, 27 (2003), ISSN 0370-2693, URL <http://www.sciencedirect.com/science/article/pii/S0370269303000984>.
- [21] K. Perajarvi *et al.*, Phys. Rev. C **74**, 024306 (2006).
- [22] Z. Yong-Nan, Z. Dong-Mei, Y. Da-Qing, Z. Yi, F. Ping, M. Mihara, K. Matsuta, M. Fukuda, T. Minamisono, T. Suzuki, et al., Chinese Physics Letters **27**, 022102 (2010), URL <http://stacks.iop.org/0256-307X/27/i=2/a=022102>.
- [23] D. W. Lee, J. Powell, K. Perjarvi, F. Q. Guo, D. M. Moltz, and J. Cerny, Journal of Physics G: Nuclear and Particle Physics **38**, 075201 (2011), URL <http://stacks.iop.org/0954-3899/38/i=7/a=075201>.
- [24] M.F. Jager *et al.*, Phys. Rev. C **86**, 011304(R) (2012).
- [25] L.G. Sobotka *et al.*, Phys. Rev. C **87**, 054329 (2013).
- [26] F. Ajzenberg-Selove, Nuclear Physics A **506**, 1 (1990), ISSN 0375-9474, URL <http://www.sciencedirect.com/science/article/pii/037594749090271M>.
- [27] K.A. Chipps *et al.*, Nucl. Instr. and Methods A **763**, 553 (2014).
- [28] D. W. Bardayan, J. C. Blackmon, W. Bradfield-Smith, C. R. Brune, A. E. Champagne, T. Davinson, B. A. Johnson, R. L. Kozub, C. S. Lee, R. Lewis, et al., Phys. Rev. C **63**, 065802 (2001), URL <http://link.aps.org/doi/10.1103/PhysRevC.63.065802>.
- [29] O. Tengblad and C. Aa. Diget, Hyperfine Interact. **223**, 81 (2014).